Environ Monit Assess (2020) 192: 100
https://doi.org/10.1007/s10661-020-8062-3

Analysis of the effect of inputs uncertainty on riverine water temperature predictions with a Markov chain Monte Carlo (MCMC) algorithm

Babak Abdi · Omid Bozorg-Haddad · Hugo A. Loáiciga

Received: 31 January 2019 / Accepted: 1 January 2020 / Published online: 8 January 2020

Abstract Water temperature is a key characteristic defining chemical, physical, and biologic conditions in riverine systems. Models of riverine water quality require many inputs, which are commonly beset by uncertainty. This study presents an uncertainty analysis of inputs to the stream-temperature simulation model HFLUX. This paper's assessment relies on a Markov chain Monte Carlo (MCMC) analysis with the DREAM algorithm, which has fast convergence rate and good accuracy. The inputs herein considered are the river width and depth, percent shade, view to sky, streamflow, and the minimum and maximum values of inputs required for uncertainty analysis. The results are presented as histograms for each input specifying the input's uncertainty. A comparison of the observational data with the DREAM algorithm estimates yielded a maximum error equal to 7.5%, which indicates excellent performance of the DREAM algorithm in ascertaining the effect of uncertainty in riverine water quality assessment.

B. Abdi · O. Bozorg-Haddad (✉)
Department of Irrigation & Reclamation Engineering, Faculty of Agricultural Engineering & Technology, College of Agriculture & Natural Resources, University of Tehran, Karaj, Tehran, Iran
e-mail: OBHaddad@ut.ac.ir

B. Abdi
e-mail: Babak.Abdi@ut.ac.ir

H. A. Loáiciga
Department of Geography, University of California, Santa Barbara, CA 93016-4060, USA
e-mail: Hugo.Loaiciga@geog.ucsb.edu

Keywords Uncertainty · DREAM algorithm · MCMC algorithm · HFLUX simulation

Introduction

Hydrologic simulation models feature multiple parameters whose specification may be uncertain in many applications. Such parameter uncertainties are propagated to the simulations' outputs. Methods for assessing the uncertainty of simulation models commonly rely on specialized algorithms that determine the most probable values on uncertain model inputs. Kamali et al. (2012) employed the particle swarm optimizer (PSO) to evaluate the effect of parameters in Hydrologic Engineering Center's hydrologic Modeling System (HEC-HMS) simulations. The PSO obtained the most probable values of the HEC-HMS model parameters with fast search convergence. Yang et al. (2008) compared the Markov chain Monte Carlo (MCMC), the generalized likelihood uncertainty estimation (GLUE), the sequential uncertainty fitting (SUFI)2, and the parameter solution (ParaSol) uncertainty methods to assess the uncertainty of hydrologic simulations in a region of China. The results demonstrated variable convergences of the compared methods in the parameter space. Nkonge et al. (2014) compared the SUFI2 and GLUE algorithms' effectiveness in reducing the impacts of parameter uncertainty in the analysis of flooding in the Tana region of Kenya. The SUFI2 algorithm was found superior to the GLUE algorithm in reducing the effect of parameter uncertainty in their study. Shen et al. (2012) linked the

GLUE uncertainty analysis algorithm and the soil water assessment tool (SWAT) for hydrologic simulation and analyzed the effect of uncertainty of the SWAT parameters in predictions of sediment transport and flow simulations during heavy precipitation, and their study's showed that sediment simulation presented greater uncertainty than stream flow, and uncertainty was even greater in high precipitation conditions (from May to September) than during the dry season. Alazzy et al. (2015) applied the GLUE algorithm to assess the uncertainty of simulations with the Xinanjiang rainfall-runoff (XAJ-RR) model. The results highlighted the key role that the model's parameters' uncertainty has on runoff simulations.

Markov chain Monte Carlo (MCMC) algorithms are widely used in uncertainty analysis. These algorithms generate random samples using Markov chains for the analysis of uncertainty. Tuning automatically the scale and orientation of the proposed distribution to derive the target distribution and exhibiting excellent sampling efficiencies on complex, high-dimensional, and multimodal target distributions are these algorithms' key advantages (Vrugt 2016). The disadvantage of the MCMC algorithms arises from the initial random samples that may follow a poorly fitted distribution. One variant of the MCMC algorithms is the DiffeRential Evolution Adaptive Metropolis (DREAM) algorithm (Vrugt et al. 2008, 2009; Shojai 2012). The speed and precision convergence of the DREAM has been demonstrated in several studies and proven superior to other adaptive MCMC sampling approaches (Vrugt 2016). Shojai (2012) employed the DREAM algorithm to assess the effective parameters of the QUAL-2 K riverine water quality model. Koskela et al. (2012) applied the DREAM algorithm to evaluate the effect of parameters' uncertainty on predictions by the identification of unit hydrographs and component flows from rainfall, evapotranspiration, and streamflow (IHACRES) simulation model; their study's result showed that occasional snow water equivalent (SWE) observations together with daily streamflow observations do not contain enough information to simultaneously identify model parameters, precipitation uncertainty, and model structural uncertainty. Zheng and Han (2016) evaluated the uncertainty of simulations of watershed-scale water quality (WWQ) model with the DREAM algorithm. Their study showed the MCMC UA has to be management-oriented, that is, management objectives must be factored into the design of the UA rather than be considered after the UA. Joseph and Guillaume (2013) employed the DREAM algorithm to identify likelihood functions of SWAT simulations. Hydrologic simulation models require diverse inputs, among which are parameters, environmental data, boundary and initial conditions, spatial geometry, and the like. Liu et al. (2017) developed a Bayesian-based multilevel factorial analysis (BMFA) method to assess parameter uncertainties and their effects on hydrological model responses. In their study, the DREAM algorithm was applied to the analysis of parameter uncertainty. The uncertainties of four sensitive parameters, including soil conservation service runoff curve number to moisture condition II (CN2), soil hydraulic conductivity (SOL_K), plant available water capacity (SOL_AWC), and soil depth (SOL_Z), were investigated, and their findings indicate that significant parameters and their statistical associations can be quantified. Farsi and Mahjouri (2019) evaluated the impacts of human activities and climate change on river flow. They applied the DREAM algorithm for analyzing the model parameters uncertainty. Their findings demonstrated the parameters of LSMX (maximum moisture capacity of the lower soil layer), and K3 (deep percolation coefficient) are the most significant parameters controlling the uncertainty of simulated runoff. Nourali et al. (2016) investigated the uncertainty of parameters of the HEC-HMS model with the DREAM algorithm with both formal and informal likelihood functions. Also, the performance of seven different likelihood functions (L1–L7) was assessed with the DREAM approach. Results showed the DREAM algorithm performed better under formal likelihood functions L5 and L7. Leta et al. (2015) adapted a method to incorporate rainfall uncertainty in distributed hydrologic models. Their study considered different sources of uncertainty in semi-distributed hydrologic model and implemented the DREAM algorithm to infer the parameter posterior distributions and the output uncertainties of the SWAT model. Leta et al. (2015) found that considering heteroscedasticity and rainfall uncertainty leads to more realistic parameter values, better representation of water balance components, and prediction uncertainty intervals. Aghakhani Afshar et al. (2019) investigated the application of parameter uncertainty quantification methods and their performance for predicting runoff. Their study implemented the DREAM algorithm for the analysis of the output uncertainty of the Soil and Water Assessment Tool (SWAT) model. Their study result showed the DREAM-ZS algorithm improved the model calibration efficiency and led to more realistic values of the parameters for

runoff simulation with the SWAT model. Liang et al. (2016) evaluated the effect of water quality model parameter uncertainty on TMDLs. They employed the DREAM algorithm for the model parameter uncertainty analysis, and an allowable pollutant load calculation platform was established with the Environmental Fluid Dynamics Code (EFDC), which is a widely applied hydrodynamic-water quality model.

This study links the DREAM uncertainty analysis algorithm and the HFLUX simulation model for the purpose of ascertaining the effect of inputs uncertainty on model's predictions of stream water temperature. The probability distribution functions of selected model inputs are calculated, and their effect on model predictions is evaluated. Figure 1 depicts the steps of this paper's methodology, where it is seen the first step is the selection of the simulation model. Changes in the simulation model linked to the DREAM algorithm are applied leading to the assessment of the effect of inputs' uncertainties on model simulations. The observational data are compared with model simulations to evaluate the performance of the uncertainty analysis. The HFLUX model (Glose et al. 2017) simulates riverine water temperature based on multiple inputs. It is an open-source model amenable for the type of uncertainty analysis proposed in this work.

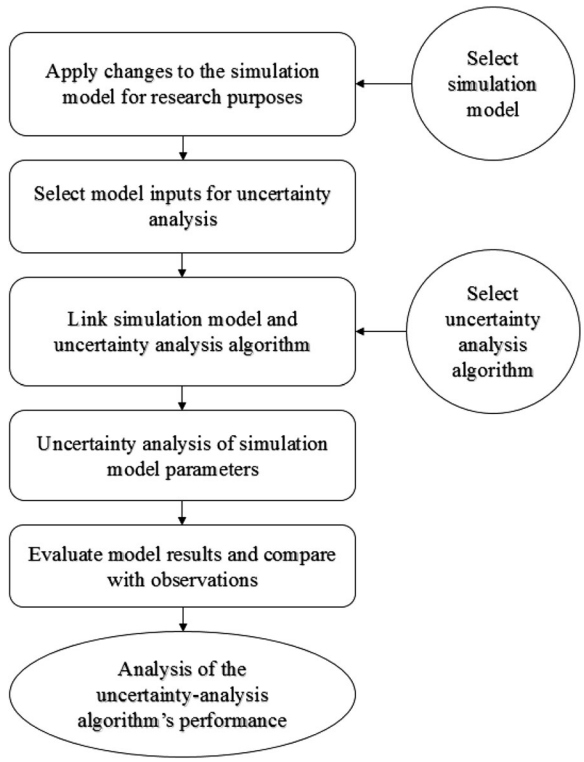

Fig. 1 The steps of this paper's methodology

Materials and methods

River water temperature: the HFLUX simulation model

Riverine water temperature is a fundamental water quality characteristic that affects the saturation of dissolved oxygen, kinetic reactions and resulting pollutant concentrations and fish distribution, metabolism, growth, reproduction, and mortality (Abdi and Endreny 2019). This work implements the HFLUX water-temperature simulation model (Glose et al. 2017) for the purpose of uncertainty analysis. HFLUX is a 1D transient model that calculates stream temperatures in space and time by solving the mass and energy balance equations for temperature transport in streams. HFLUX receives initial spatial and temporal temperature conditions, stream geometry data, discharge data, and meteorological data to calculate stream temperature employing a finite-difference solver. The HFLUX solves the water balance Eq. (1) and energy balance Eq. (2):

$$\frac{\partial A}{\partial T} + \frac{\partial Q}{\partial x} = q_L \tag{1}$$

$$\frac{\partial (AT_W)}{\partial t} + \frac{\partial (QT_W)}{\partial x} = q_L T_L + R \tag{2}$$

where A signifies the cross-sectional area of the stream (m^2), Q denotes the discharge of the stream (m^3/s), x is stream distance (m), t is time (s), q_L is the groundwater inflow per unit stream length (m^2/s), T_w is the stream temperature ($°C$), and T_L denotes the groundwater temperature ($°C$). This formulation is based on a thermal datum of 0 $°C$ governs the absolute value of the advective heat flux term. The first term on the right-hand side of Eq. (2) becomes $q_L T_w$ if q_L is negative, which indicates a losing stream. Also, in this Eq., R signifies the energy flux (source or sink) per unit stream length that is calculated based on Eq. (3):

$$R = \frac{B\varphi_{total}}{\rho_w C_w} \tag{3}$$

where B denotes the width of the stream (m), φ_{total} represents the total energy flux to the stream per surface

area (W/m^2), ρ_w denotes the density of water (kg/m^3), and C_w is the specific heat of water (J/kg°C). Dispersive heat transport is negligible where water temperature longitudinal change is small in comparison to temporal changes. Dispersive transport is omitted in Eq. (2). Equations (1) and (2) are solved numerically with an open-source MATLAB script that can be downloaded at no cost from http://hydrology.syr.edu/hflux. Figure 2 depicts the steps of this simulation model. Accordingly, the model first receives the required inputs and solves the water and energy balance equations at the nodes representing the numerical longitudinal discretization of the stream length for all time steps of the simulation.

HFLUX model inputs include meteorological data, river geometric data, temperature initial conditions, spatial conditions, and discharge data. The data employed in this work's uncertainty analysis corresponds to June 13–19, 2012 (Glose et al. 2017).

The DREAM uncertainty algorithm

The DREAM algorithm is a variant of the generic MCMC algorithms that has proven efficient in the assessment of parameter and predictive uncertainty and experimental design (Vrugt et al. 2009, 2011). The DREAM algorithm has been proven superior to other MCMC algorithms in previous studies and has yielded accurate solutions in high-dimensional search/variable spaces (Vrugt 2016). The DREAM algorithm iterates by generating chains of d-dimensional candidate vectors z^i from the current values of vectors $\boldsymbol{x}$, $i = 1, 2, \ldots, N$, where N denotes the number of vectors considered by the DREAM algorithm, and d is the number of evaluated parameters or inputs in each vector. The DREAM algorithm convergence to stationary or limiting distributions of parameters after repeated iterations has been found to be faster than those of traditional MCMC algorithms (Vrugt 2016). The generation of candidate vector z^i from current vector x^i in the i-th iteration ($i = 1, 2, \ldots, N$) is accomplished with the following equation (Vrugt and Ter Braak 2011):

$$z^i = x^i + (1_d + e_d)\gamma\left(\delta, d'\right)\left(\sum_{j=1}^{\delta} x^{r_1(j)} - \sum_{n=1}^{\delta} x^{r_2(n)}\right) + \varepsilon_d \quad (4)$$

where z^i is the candidate vector and x^i is the current vector (of parameters or inputs variables); e_d and ε_d are drawn from $U_d(-b, b)$ [d-variate uniform distribution in

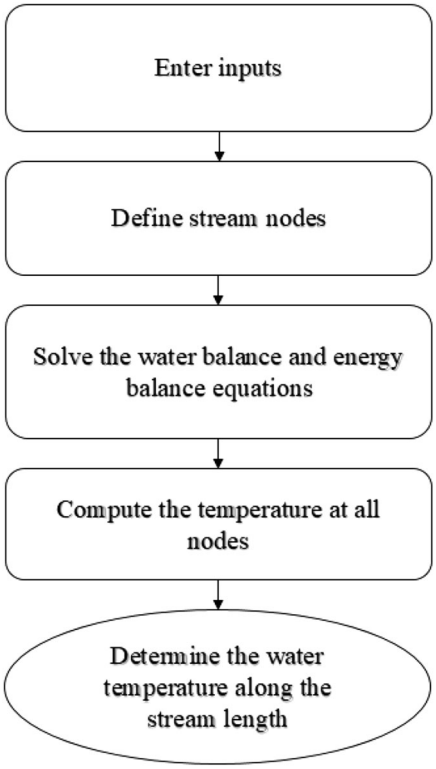

Fig. 2 The steps of the HFLUX simulation model

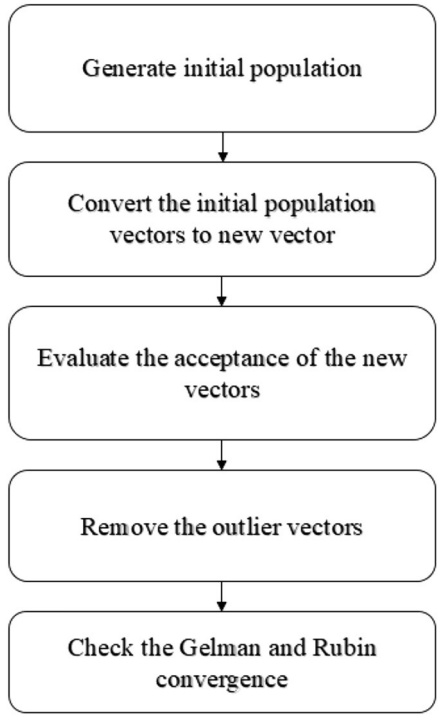

Fig. 3 The steps of the DREAM algorithm

$(-b, b)$], typically, $b = 0.1$, and $N_d(0, b^*)$ denotes the d-variate normal distribution with zero mean and variance b^* small compared to the variance of the target distribution; δ is the number of pairs used to generate the candidate vector; γ denotes the value of the jump size, which depends on δ and d', the number of dimensions updated jointly in an iteration step. A good choice is $\gamma = 2.4/\sqrt{2\delta d'}$ (Vrugt and Ter Braak 2011); $x^{r_1(j)}$ and $x^{r_2(n)}$ are randomly selected without replacement from the population of vectors x without x^i; $r_1(j)$ and $r_2(n)$ are in the range [1, 2,…, N]. Replace the j-th (Z^i_j) chain of the generated candidate vector z^i according to the following criterion to create a new vector ($j = 1, 2,\ldots, d$):

$$Z^i_j = \begin{cases} x^i_j & if \quad U \le 1-CR \\ z^i_j & otherwise \end{cases} \tag{5}$$

where CR is the crossover probability and U is drawn from a uniform distribution $U \in [0, 1]$.

The next step of the DREAM algorithm computes $\pi(Z^i)$ and accepts the new vector Z^i with Metropolis acceptance probability, $\alpha(x^i, Z^i)$:

$$\alpha\left(x^i, Z^i\right) = \begin{cases} \min\left(\dfrac{\pi(Z^i)}{\pi(x^i)}\right), 1 & if\ \pi\left(x^i\right) > 0 \\ 1 & if\ \pi\left(x^i\right) = 0 \end{cases} \tag{6}$$

If the new vector is accepted, $Z^i = x^i$; otherwise, it remains at the old location x^i. The next step removes the potential outlier vectors using the interquartile range (IQR) statistic. The outlier vectors can significantly deteriorate the performance of MCMC samplers and must be removed to facilitate convergence to a limiting distribution. The final step of the DREAM algorithm is evaluating the Gelman and Rubin convergence diagnostic. This diagnostic compares for each parameter the within-chain:

$$W_j = \frac{2}{N(T-2)} \sum_{i=1}^{N} \sum_{r=[T/2]}^{T} \left(x^i_{r,j} - \overline{x}^{\,i}_j\right)^2 \tag{7}$$

in which

$$\overline{x}^{\,i}_j = \frac{2}{T-2} \sum_{r=[T/2]}^{T} x^i_{r,j} \tag{8}$$

and between-chain variance

$$B_j/T = \frac{1}{2(N-1)} \sum_{i=1}^{N} \left(\overline{x}^{\,i}_j - \overline{x}_j\right)^2 \tag{9}$$

in which

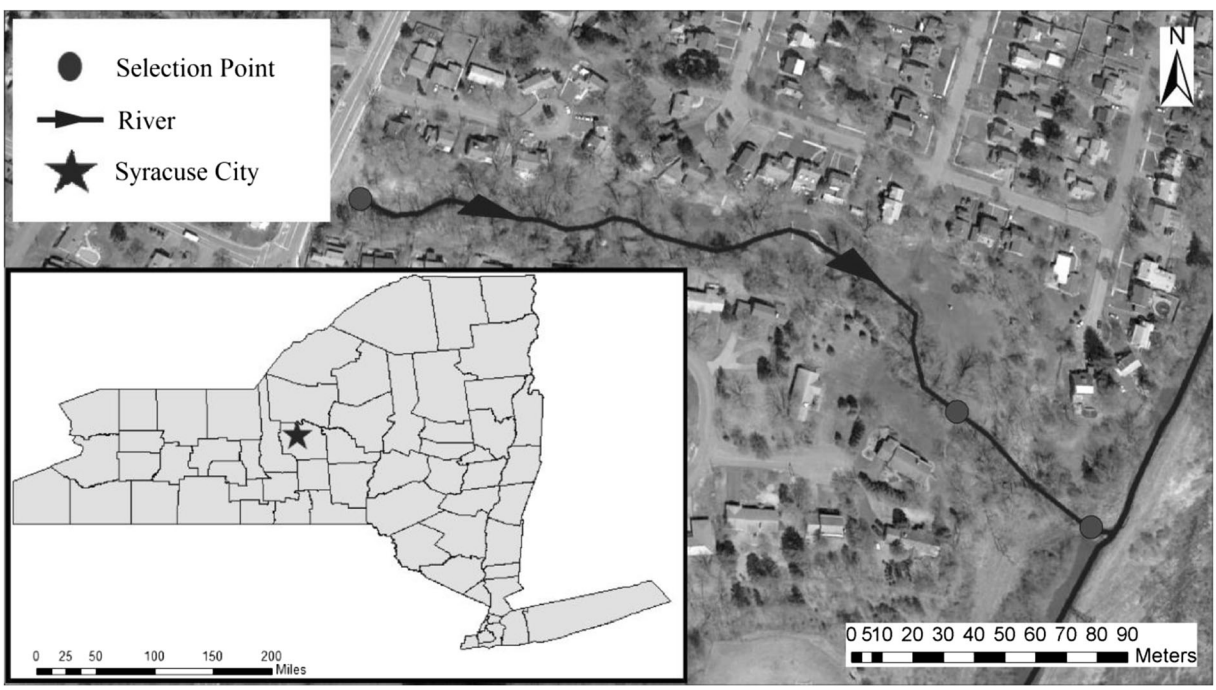

Fig. 4 The study region and location of the 3 nodes (the gray map represents the state of New York)

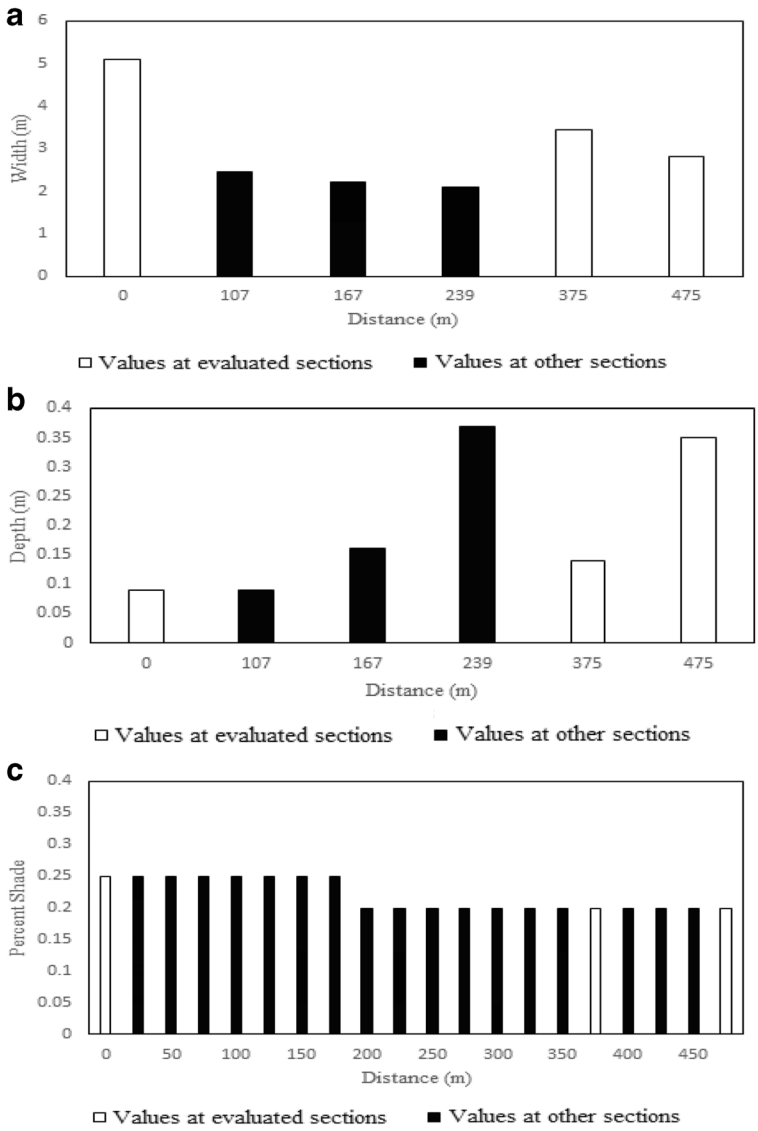

Fig. 5 Graphs of the values at several sections along Meadowbrook Creek (**a**) creek width, (**b**) creek depth, (**c**) percent shade, (**d**) view to sky, and (**e**) discharge

$$\bar{\bar{x}}_j = \frac{1}{N}\sum_{i=1}^{N} \bar{x}_j^i \tag{10}$$

where

$$\sigma_+^{2(j)} = \frac{T-2}{T} W_j + \frac{2}{T} B_j \tag{11}$$

and defining

$$R_j = \sqrt{\frac{N+1}{N}\frac{\sigma_+^{2(j)}}{W_j} - \frac{T-2}{NT}} \tag{12}$$

where T signifies the number of samples in each chain, $r = \{1, ..., T\}$, $\lfloor . \rfloor$ is the integer rounding operator, $x_{i,j}^r$ is the parameter value at j-th dimension, i-th vector, and r-th sample, $\sigma_+^{2(j)}$ is an estimate of the variance of the j-th parameter of the target distribution, and R_j is the value of this diagnostic. The value of R_j must be less than 1.2 for all parameters. Figure 3 depicts the steps of the DREAM algorithm. Accordingly, the algorithm iterates by generating initial population of N vectors with dimension d. According to Eqs. (4) and (5), each of the initial population vectors convert to new vectors. The new vectors

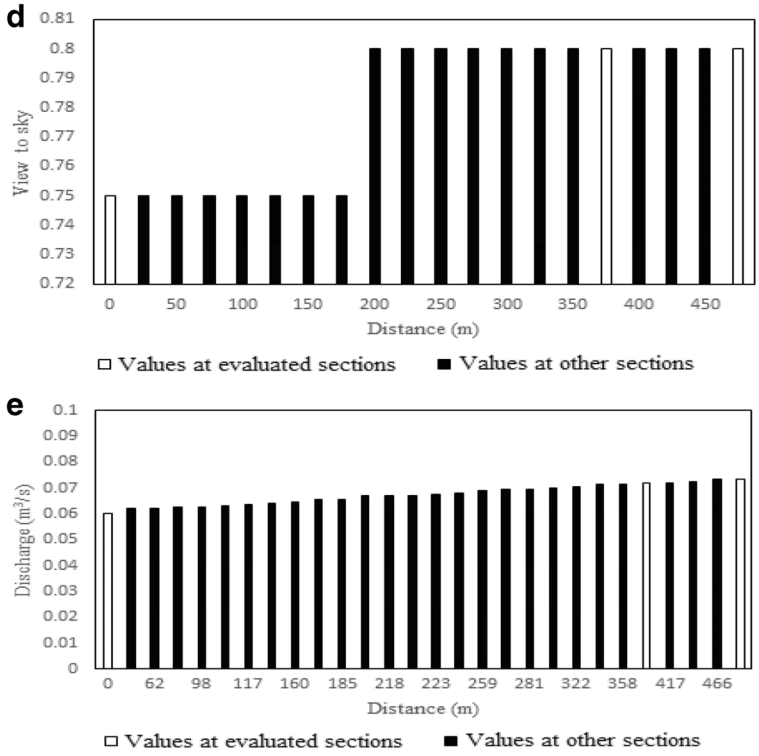

Fig. 5 continued.

acceptance is evaluated with Eq. (6). In the next step, the outlier vectors are removed, and at last, the Gelman and Rubin convergence is evaluated with Eqs. (7)–(12). The open source of the DREAM algorithm is available at the following link https://faculty.sites.uci.edu/jasper/software (Vrugt et al. 2008; Vrugt and Ter Braak 2011; Vrugt 2016).

Table 1 The HFLUX selected inputs and their upper and lower limits specified in the uncertainty analysis

Input	Description	Minimum	Maximum	Unit
W_1	River width at the beginning of the river (0 m)	1	7	m
W_2	River width at 375 m from the beginning of the river	1	7	m
W_3	River width at the end of the river (475 m)	1	7	m
D_1	River depth at the beginning of the river	0.001	1	m
D_2	River depth at 375 m from the beginning of the river	0.001	1	m
D_3	River depth at the end of the river	0.001	1	m
Sh_1	Shade coefficient at the beginning of the river	0	1	–
Sh_2	Shade coefficient at 375 m from the beginning of the river	0	1	–
Sh_3	Percent hade coefficient at the end of the river	0	1	–
V_1	View to sky coefficient at the beginning of the river	0	1	–
V_2	View to sky coefficient at 375 m from the beginning of the river	0	1	–
V_3	View to sky coefficient at the end of the river	0	1	–
Q_1	Discharge river at the beginning of the river	0.05	0.1	m^3/s
Q_2	Discharge river at 375 m from the beginning of the river	0.05	0.1	m^3/s
Q_3	Discharge at the beginning of the river	0.05	0.1	m^3/s

The study region

The study region is the urban Meadowbrook Creek catchment within the city of Syracuse, state of New York (Glose et al. 2017). Meadowbrook creek is a first-order stream with a catchment area equal to 6.3 km^2 covered by residential, industrial, and open spaces, which meanders through the city of Syracuse. The creek serves fishing, recreational, and tourism uses. The creek's length equals four kilometers, of which 475 m are herein simulated for water temperature at three selected points shown in Fig. 4. The reason of choosing these three points is the identical sampling of the selected inputs at these points. Also, the changes of inputs values relative to each other at these points are greater than at other points thus permitting improved evaluation of the algorithm performance. Creek discharge variations during the observational period (June 13–19, 2012) fell in the range of 0.06–0.63 (m^3/s) and increases nearly linearly with increasing downstream distance. Daily temperature in the observational period (June 13–19, 2012) ranged between 8.9 and 28.2 ($°C$). The maximum and minimum relative humidity varied in the range of 36–93%. The channel sediments consist of cobbles, clay, sand, and gravel, clay being the predominate soil type. The urban landscape and local precipitation exert a primary control on stream flow and water-quality characteristics.

Results and discussion

The inputs to the HFLUX model selected for uncertainty analysis in this study include the depth and width of the river, percent shade**,** view to sky, and creek discharge in three distinct sections of the creek comprised within a 475 m reach shown in Fig. 4. An uncertainty analysis of the selected HFLUX inputs and model predictions was conducted by coupling HFLUX to the DREAM algorithm. Figure 5 displays the values of selected inputs along the study reach.

The DREAM algorithm was implemented to determine the posterior distribution function of the selected inputs. The initial population of inputs was specified from the minimum and maximum values for each input based on field observations and known likely ranges for each input in the study area. DREAM calculates the posterior distribution functions of the selected inputs and draws values from these posterior distributions to be input to HFLUX. The selected inputs and their minimum and maximum values are listed in Table 1.

Creek flow and water temperature were simulated with HFLUX employing a spatial step equal to 10 m and time step equal to 30 min. The DREAM algorithm iterated 55,000 times in $N = 3$ vector in the uncertainty analysis. Acceptance of the DREAM-calculated probability distributions of selected inputs was based on the Gelman and Rubin convergence criteria (Gelman and Rubin 1992), which in this work establishes this

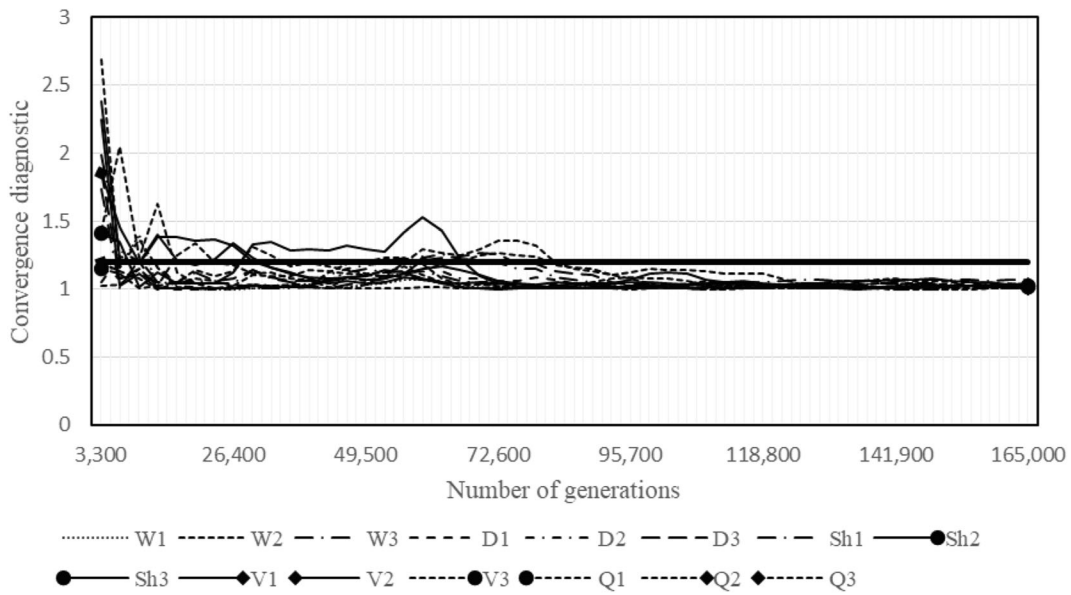

Fig. 6 Gelman and Rubin criterion chart for the model inputs

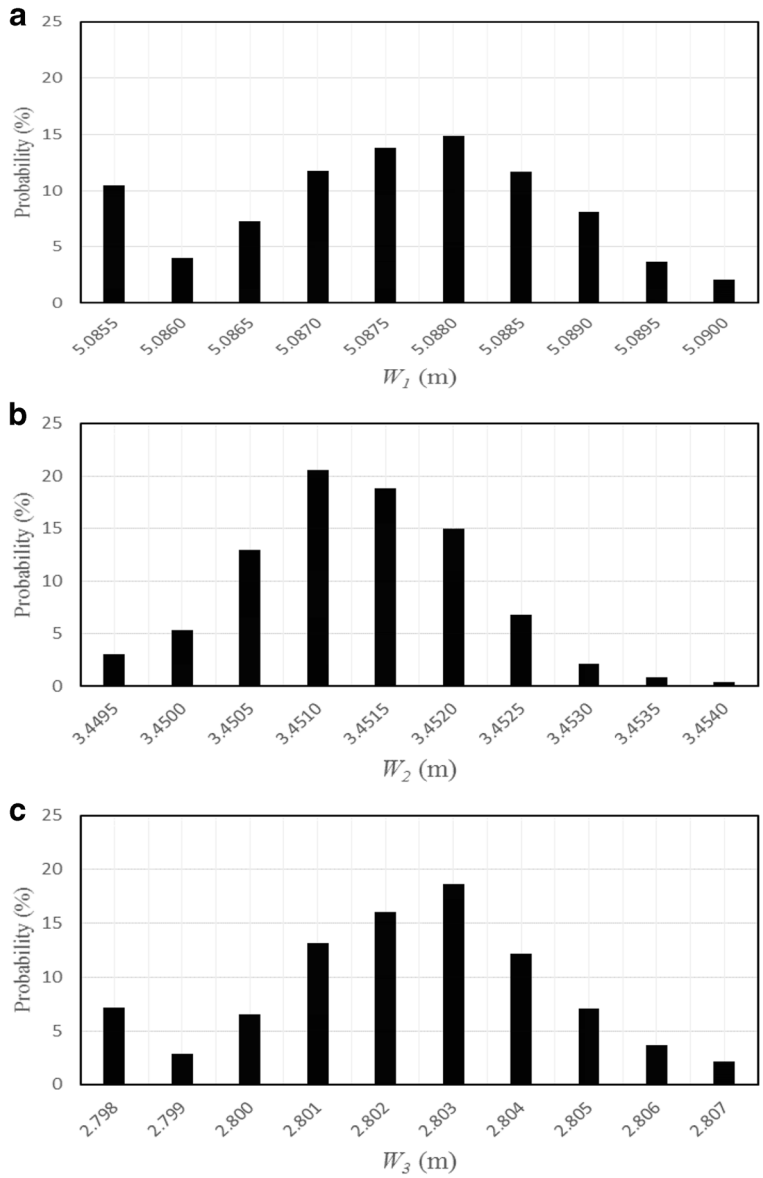

Fig. 7 The histogram of HFLUX inputs at three sections (**a**) creek width at the beginning of reach (0 m), (**b**) creek width at 375 m from the beginning of the reach, and (**c**) creek width at the end of the each (475 m)

convergence for selected inputs must have a criterion less than 1.2 at the end of iterations, as shown in Fig. 6, where the Gelman and Rubin convergence for all the selected inputs at the end of iteration have a criterion less than 1.2.

The posterior distribution functions for each of the selected inputs were calculated and are represented as histograms after linking the DREAM uncertainty algorithm and the HFLUX simulation model in the uncertainty analysis. The width of the range of the posterior distribution function of the selected inputs measures the uncertainty of an input: the wider the range, the more uncertain the input. The average value or the most likely value of the posterior distribution of an input are identified by the DREAM algorithm as suitable values for that input to carry out simulations of stream water quality. The calculated posterior distribution functions for the selected inputs produced by the linked DREAM algorithm and HFLUX model are displayed in Figs. 7, 8, 9, 10, and 11. It is seen in Figs. 7, 8, 9, 10, and 11 the posterior distributions of selected model inputs are not symmetric. According to the Fig. 7, the uncertainty range of the width of the stream at the first location is between 5.0880 and 5.09, and the most likely value

predicted by DREAM equals 5.088. The uncertainty range for this input at the second location is 3.4495 through 3.454 and most likely value equal to 3.451. The range for the third location is 2.798 through 2.807 with most likely value equal to 2.803. According to the Fig. 8, the uncertainty range of the depth of the stream at the first location is 0.09011 through 0.0902 with most likely value predicted by DREAM equal to 0.09017. The uncertainty range for this input at the second location is 0.1396 through 0.14005 with most likely value equal to 0.13975. The range for the third location is 0.3498 through 0.3507 with most likely value equal to 0.3502. According to Fig. 9, the uncertainty range of the percent shade coefficient at the first location is 0.2444 through 0.2465 with most likely value predicted by DREAM equal to 0.2453. The uncertainty range for this input at the second location is 0.203 through 0.2075 with most likely value equal to 0.2045. The range for the third location is 0.193 through 0.202 with most likely value equal to 0.199. According to Fig. 10, the uncertainty range of the view to sky coefficient at the first location is 0.7413 through 0.753 with most likely value predicted by DREAM equal to 0.7465. The uncertainty range for this input at the second location is 0.84 through 0.876 with most likely value equal to 0.86. The range for the third location is 0.75 through 0.795

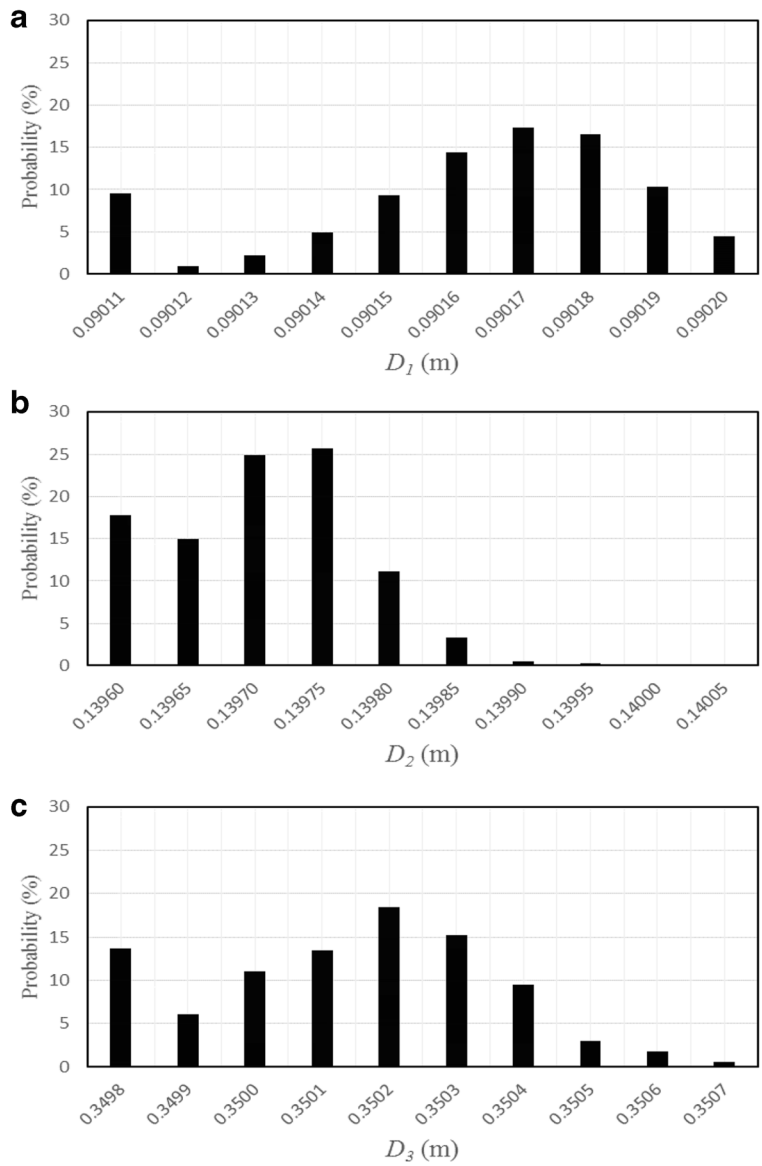

Fig. 8 The histogram of HFLUX inputs at three sections (**a**) creek depth at the beginning of the reach, (**b**) creek depth at 375 m from the beginning of the reach, and (**c**) creek depth at the end of the reach

with most likely value equal to 0.77. According to the Fig. 11, the uncertainty range of the discharge coefficient at the first location is 0.060303 through 0.060312 with most likely value predicted by DREAM equal to 0.060308. The uncertainty range for this input at the second location is 0.07187 through 0.071915 with most likely value equal to 0.07189. The range at the third location is 0.07336 through 0.073405 with most probable value equal to 0.07339.

The coefficient of variation of an input measures its spread about its mean value. The lower the coefficient of variation, the higher the sensitivity of the simulation model to an input. Table 2 lists the coefficient of variation of each of the input estimated by the DREAM algorithm. It is seen in Table 2 the input Q_1 with the coefficient of variation 0.71% is the most sensitive input, and the inputs Q_2 and Q_3 are the second and third most sensitive, respectively.

The most probable values estimated by the DREAM algorithm for each input were compared with the observed values. Table 3 lists the DREAM estimation error, where it is seen the largest error corresponds to input V_2 with 7.5% error. The estimates of the DREAM algorithm for W_2 with 0.03% error was the smallest. The

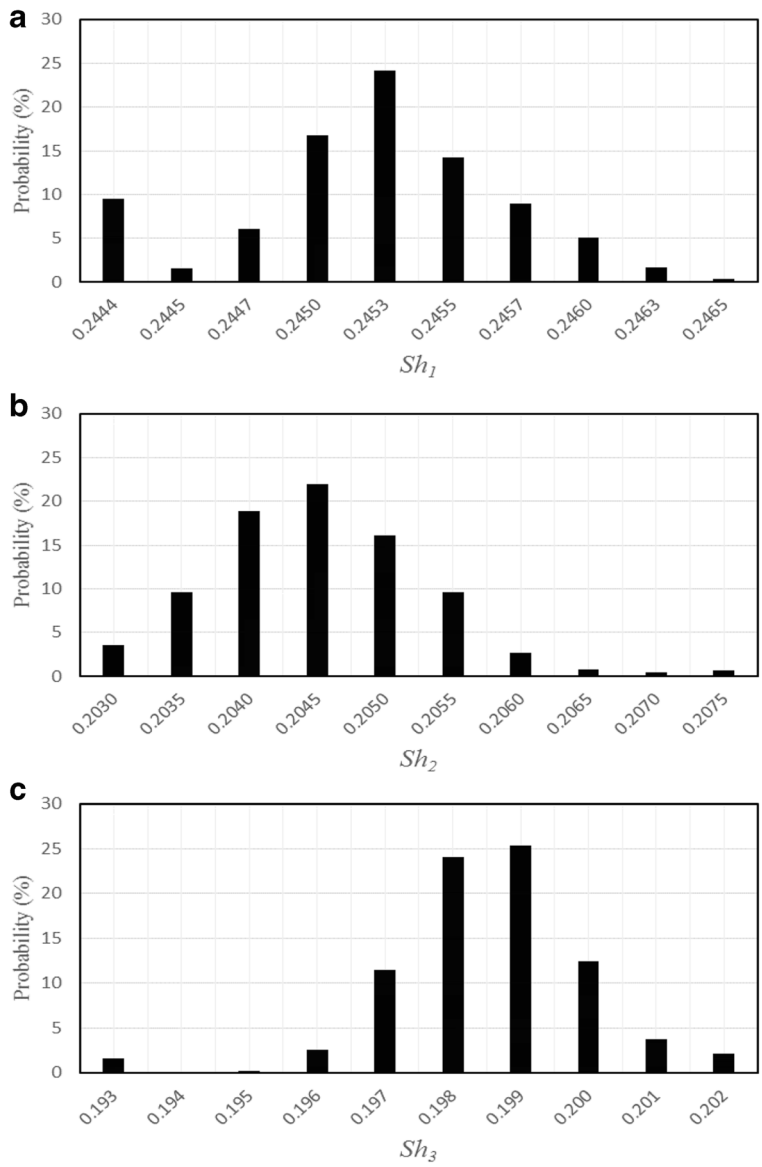

Fig. 9 The histogram of HFLUX inputs at three sections (**a**) percent shade coefficient at the beginning of the reach, (**b**) percent shade coefficient at 375 m from the beginning of the each, and (**c**) percent shade coefficient at the end of the reach

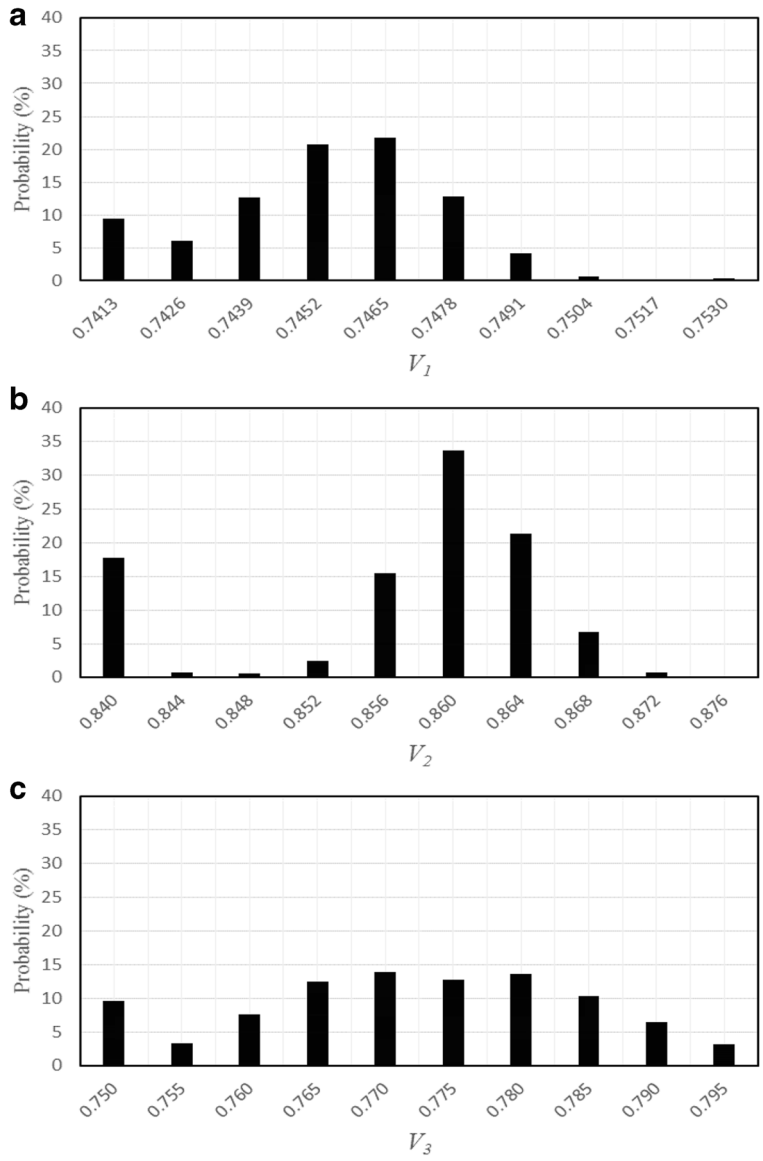

Fig. 10 The histogram of HFLUX inputs at three sections (**a**) view to sky coefficient at the beginning of the reach, (**b**) view to sky coefficient at 375 m from the beginning of the reach, and (**c**) view to sky coefficient at the end of the each

fact that the largest estimation error with the DREAM algorithm is 7.5% is testimony to its good performance.

Conclusion

This paper assessed the uncertainties of the inputs to the HFLUX stream water-quality model linked to the DREAM MCMC algorithm. The Meadowbrook River, Syracuse, New York, USA, was chosen as the case study. The results of the uncertainty assessment of HFLUX model inputs are presented in the form of histograms or empirical distribution functions that represent the uncertainty and most likely values for each model input at selected river nodes. The width of the range of these histograms measures the uncertainty of each of the model inputs. Accordingly, the input Sh_2 with largest width of the histogram and with a coefficient of variation equal to 63.43% is the most uncertain. The input Q_1 with smallest width of histogram range and a coefficient of variation equal to 0.71% is the least uncertain. Our results indicate the input Q_1 is the most sensitive input, and the input Sh_2 is the least sensitive input. The mean or the most likely value of the posterior distribution function obtained for each of the inputs by the DREAM analysis algorithm may be used for stream

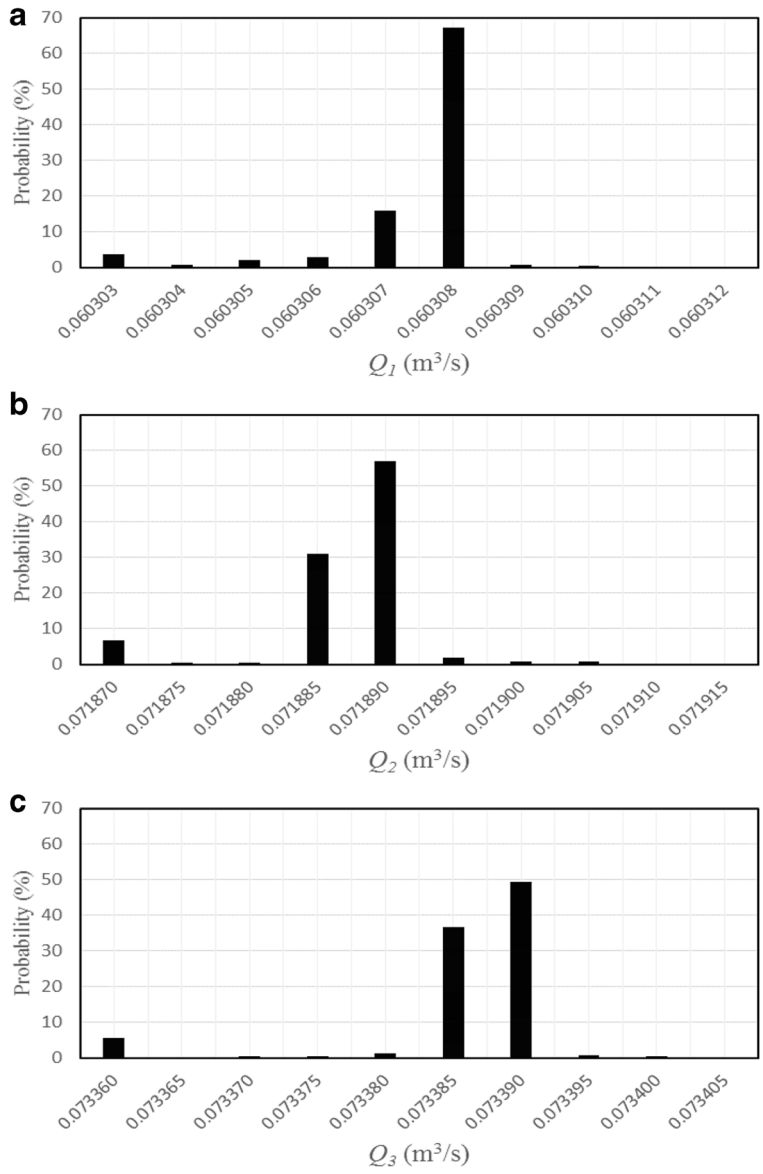

Fig. 11 The histogram of HFLUX input at three sections (**a**) discharge coefficient at the beginning of the reach, (**b**) discharge coefficient at 375 m from the beginning of the each, and (**c**) discharge coefficient at the end of the reach

Table 2 The inputs' coefficient of variation

Input	Coefficient of variation (percentage)	Input	Coefficient of variation (percentage)
W1	6.56	*Sh3*	46.53
W2	7.51	*V1*	6.91
W3	20.43	*V2*	19.51
D1	61.83	*V3*	17.38
D2	28.21	*Q1*	0.71
D3	13.38	*Q2*	0.81
Sh1	15.38	*Q3*	1.02
Sh2	63.43		

quality simulations. These results and the observational data indicate the input W_2 with the smallest estimation error of the most likely value of the posterior distribution function equal to 0.03% is the most accurately estimated input, and the input V_2 with the largest error in estimating the most likely value of the posterior distribution function equal to 7.5% is the least accurately estimated input. The closeness of the model predictions and observational values demonstrates suitable performance of the DREAM algorithm for identifying optimal model inputs.

Table 3 The estimation errors produced by the DREAM algorithm

Input	Error (percentage)	Input	Error (percentage)
W1	0.24	*Sh3*	0.5
W2	0.03	*V1*	0.47
W3	0.11	*V2*	7.5
D1	0.19	*V3*	3.75
D2	0.18	*Q1*	0.13
D3	0.06	*Q2*	0.13
Sh1	1.88	*Q3*	0.18
Sh2	2.25		

Acknowledgments The authors thank Iran's National Science Foundation (INSF) for its financial support of this research.

Compliance with ethical standards

Conflict of interests The authors declare that they have no conflict of interests.

References

Abdi, R., & Endreny, T. (2019). A river temperature model to assist managers in identifying thermal pollution causes and solutions. *Water., 11*(5), 1060.

Aghakhani Afshar, A., Hassanzadeh, Y., Pourreza-Bilondi, M., & Memarian, H. (2019). Uncertainty analysis of a continuous hydrological model using DREAM-ZS algorithm. *Journal of Science and Technology Transactions of Civil Engineering*, 2228–6160.

Alazzy, A. A., Lü, H., & Zhu, Y. (2015). Assessing the uncertainty of the Xinanjiang rainfall-runoff model: effect of the likelihood function choice on the GLUE method. *Journal of Hydrologic Engineering, 20*(10). https://doi.org/10.1061/(ASCE)HE.1943-5584.0001174.

Farsi, N., & Mahjouri, N. (2019). Evaluating the contribution of the climate change and human activities to runoff change under uncertainty. *Journal of Hydrology, 574*(2019), 872–891.

Gelman, A., & Rubin, D. B. (1992). Inference from iterative simulation using multiple sequences. *Statistical Science, 7*(4), 457–472.

Glose, A. M., Lautz, L. K., & Baker, E. A. (2017). Stream heat budget modeling with HFLUX: Model development, evaluation, and applications across contrasting sites and seasons. *Environmental Modeling & Software, 92*, 213–228.

Joseph, J. F., & Guillaume, J. H. A. (2013). Using a parallelized MCMC algorithm in R to identify appropriate likelihood functions for SWAT. *Environmental Modelling & Software, 46*, 292–298.

Kamali, B., Mousavi, S. J., & Abbaspour, K. C. (2012). Automatic calibration of HEC-HMS using single-objective and multi-objective PSO algorithms. *Hydrological Processes, 27*(26), 4028–4042.

Koskela, J. J., Croke, B. W. F., Koivusalo, H., Jakeman, A. H., & Kokkonen, T. (2012). Bayesian inference of uncertainties in precipitation-streamflow modeling in a snow affected catchment. *Water Resources Research, 48*(11). https://doi.org/10.1029/2011WR011773.

Leta, O. T., Nossent, J., Velez, C., Shrestha, N. K., Griensven, A. V., & Bauwens, W. (2015). Assessment of the different sources of uncertainty in a SWAT model of the river Senne (Belgium). *Environmental Modelling and Software, 68*(2015), 129–146.

Liang, S., Jia, H., Xu, C., Xu, T., & Melching, C. (2016). A Bayesian approach for evaluation of the effect of water quality model parameter uncertainty on TMDLs: A case study of Miyun reservoir. *Science of the Total Environment, 560–561*(2016), 44–54.

Liu, Y. R., Li, Y. P., Huang, G. H., Zhang, J. L., & Fan, Y. R. (2017). A Bayesian-based multilevel factorial analysis method for analyzing parameter uncertainty of hydrological model. *Journal of Hydrology, 553*(2017), 750–762.

Nkonge, L. K., Sang, J. K., Gathenya, J. M., & Home, P. G. (2014). Comparison of two calibration-uncertainty methods for soil and water assessment tool in stream flow modelling. *Journal of Sustainable Research in Engineering, 1*(2), 40–44.

Nourali, M., Ghahraman, B., Bilondi, M. P., & Davari, K. (2016). Effect of formal and informal likelihood functions on uncertainty assessment in a single event rainfall-runoff model. *Journal of Hydrology, 540*(2016), 549–564.

Shen, Z. Y., Chen, L., & Chen, T. (2012). Analysis of parameter uncertainty in hydrological and sediment modeling using GLUE method: A case study of SWAT model applied to three gorges reservoir region, China. *Hydrology and Earth System Sciences, 16*(1), 121–132.

Shojai, M. (2012). Development of an algorithm for joint uncertainty analysis of quantity and quality variables and parameters in river water quality simulation. M.Sc. Dissertation, Department of Civil Engineering, Iran university of Tehran, Tehran, Iran.

Vrugt, J. A. (2016). Markov chain Monte Carlo simulation using the DREAM software package: Theory, concepts, and MATLAB implementation. *Environmental Modelling and Software, 75*, 273–316.

Vrugt, J. A., & Ter Braak, C. J. F. (2011). $DREAM_{(D)}$: An adaptive Markov chain Monte Carlo simulation algorithm to solve discrete, noncontinuous, and combinatorial posterior parameter estimation problems. *Hydrology and Earth System Sciences, 15*(12), 3701–3713.

Vrugt, J. A., Ter Braak, C. J. F., Clark, M. P., Hyman, J. M., & Robinson, B. A. (2008). Treatment of input uncertainty in hydrologic modeling: Doing hydrology backward with

Markov chain Monte Carlo simulation. *Water Resources Research, 44*, W00B09. https://doi.org/10.1029/2007WR006720.

Vrugt, J. A., Ter Braak, C. J. F., Gupta, H. V., & Robinson, B. A. (2009). Equifinality of formal (DREAM) and informal (GLUE) Bayesian approaches in hydrologic modeling? *Stochastic Environmental Research and Risk Assessment, 23*(7), 1011–1026.

Yang, J., Reichert, P., Abbaspour, K. C., Xia, J., & Yang, H. (2008). Comparing uncertainty analysis techniques for a SWAT application to the Chaohe Basin in China. *Journal of Hydrology, 358*(1–2), 1–23.

Zheng, Y., & Han, F. (2016). Markov chain Monte Carlo (MCMC) uncertainty analysis for watershed water quality modeling and management. *Stochastic Environmental Research and Risk Assessment, 30*(1), 293–308.